

pubs.acs.org/synthbio Research Article

Heterologous Biosynthesis of Methanobactin from *Methylocystis* sp. Strain SB2 in *Methylosinus trichosporium* OB3b

Peng Peng, Alan A. DiSpirito, Braden J. Lewis, Joel D. Nott, and Jeremy D. Semrau*



Cite This: ACS Synth. Biol. 2024, 13, 2347–2356



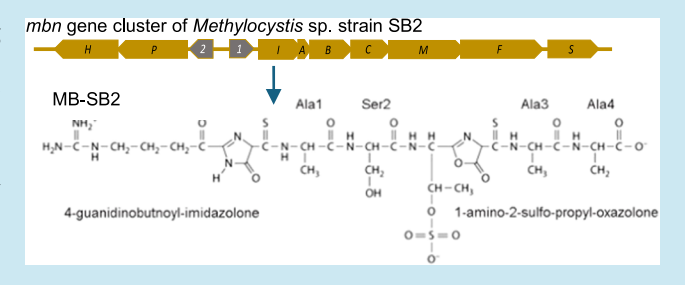
ACCESS I

III Metrics & More

Article Recommendations

s Supporting Information

ABSTRACT: Aerobic methanotrophs, or methane-consuming microbes, are strongly dependent on copper for their activity. To satisfy this requirement, some methanotrophs produce a copper-binding compound, or chalkophore, called methanobactin (MB). In addition to playing a critical role in methanotrophy, MB has also been shown to have great promise in treating copper-related human diseases, perhaps most significantly Wilson's disease. In this congenital disorder, copper builds up in the liver, leading to irreversible damage and, in severe cases, complete organ failure. Remarkably, MB has been shown to reverse such damage in animal



models, and there is a great deal of interest in upscaling MB production for expanded clinical trials. Such efforts, however, are currently hampered as (1) the natural rate of MB production rate by methanotrophs is low, (2) the use of methane as a substrate for MB production is problematic as it is explosive in air, (3) there is limited understanding of the entire pathway of MB biosynthesis, and (4) the most attractive form of MB is produced by *Methylocystis* sp. strain SB2, a methanotroph that is genetically intractable. Herein, we report heterologous biosynthesis of MB from *Methylocystis* sp. strain SB2 in an alternative methanotroph, *Methylosinus trichosporium* OB3b, not only on methane but also on methanol. As a result, the strategy described herein not only facilitates enhanced MB production but also provides opportunities to construct various mutants to delineate the entire pathway of MB biosynthesis, as well as the creation of modified forms of MB that may have enhanced therapeutic value.

KEYWORDS: methanobactin, Wilson's disease, copper

■ INTRODUCTION

Methanobactin (MB) is secreted by some aerobic methanotrophs for copper sequestration, i.e., MB is a copper-binding compound or "chalkophore" analogous to siderophores produced by many organisms for iron collection. 1,2 MBs are small (<1350 Da) ribosomally synthesized post-translationally modified polypeptides (RiPPs) that have high affinity and specificity for copper $(\sim 10^{20}-10^{30}~\text{M}^{-1})^{.1,3-12}$ To date, all identified MBs can be divided into two general groups based on structure and genetic organization, Groups I and II.^{1,13} Thus far, four Group I MBs have been characterized with the first and most extensively studied Group I MB isolated from Methylosinus trichosporium OB3b (MB-OB3b) (Figure 1A). Group I MBs are distinguished by the presence of two heterocylic rings, an oxazolone ring at the C-terminus and either another oxazolone ring at the N-terminus or in some cases, a pyrazinedione ring.^{12,13} All Group I MBs include a disulfide bridge between two cysteine residues (Figure 1A). Copper is chelated by the N- and S-ligands of the heterocyclic rings and thioamides, respectively, causing MB to form a pyramid-like shape after binding copper. 1,4,14

Four Group II MBs have also been characterized to date, with the first and most extensively examined MB being that from *Methylocystis* sp. strain SB2 (MB-SB2; Figure 1B). Group

II MBs, like Group I MBs, have two heterocyclic rings, with the C-terminal ring being an oxazolone ring. Unlike Group I MBs, however, the N-terminal ring has never been found to be another oxazolone ring; rather, it is either an imidazolone ring (as shown in Figure 1B for MB-SB2) or a pyrazinedione ring. Further, the disulfide bridge found in Group I MBs is absent from Group II MBs, and instead, these MBs are sulfonated. Evidence indicates that the addition of a sulfate group adjacent to the C-terminal oxazolone ring serves to enhance copper binding and also allows Group II MBs to form a hairpin-like structure after binding copper via the N-ligand of the oxazolone/imidazolone and S-ligand of thioamides.^{1,8}

The genetics and biochemistry of Group I MBs have been relatively well-characterized, largely through the examination of MB from *M. trichosporium* OB3b, as this strain is genetically tractable. That is, from a suite of knockout assays, it has been shown that (1) the MB precursor polypeptide is encoded by

Received: January 15, 2024 Revised: June 5, 2024 Accepted: July 26, 2024 Published: August 7, 2024





Figure 1. Primary structures of methanobactin from (A) M. trichosporium OB3b and (B) Methylocystis sp. strain SB2.

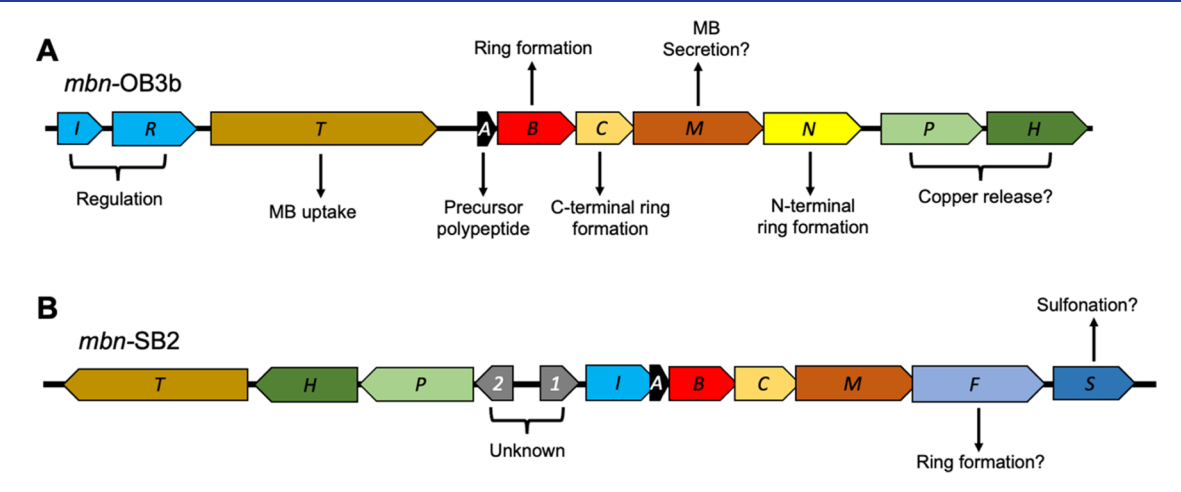


Figure 2. (A) mbn gene cluster of M. trichosporium OB3b and (B) Methylocystis sp. strain SB2. Note that functions of some gene products have yet to be experimentally determined and are indicated by a question mark.

mbnA, (2) the formation of the N-terminal oxazolone ring of MB-OB3b requires activity of a specific aminotransferase encoded by mbnN, (3) the formation of the C-terminal oxazolone ring involves the activity of the gene product of mbnC, (4) the uptake of MB-OB3b requires a TonBdependent transporter encoded by mbnT, and (5) mbnI and mbnR play key roles in controlling mbn gene expression^{6,15–19} (Figure 2A). Some evidence also suggests that mbnB plays a role in ring formation, but this was not based on genetic manipulation of M. trichosporium OB3b but rather by heterologous expression of both mbnB and mbnC in Escherichia coli. 20 Bioinformatic analyses suggest that mbnM is involved in MB secretion, but this has yet to be experimentally verified. Little is known as to the role(s) of mbnPH, i.e., mbnH encodes for a MauG-type diheme cytochrome c peroxidase²¹⁻²⁶ while its partner protein, mbnP, is a metallo-mystery four-cysteine motif protein. It has been speculated that the product of these genes may be involved in the release of copper from MB after it is reinternalized, but this has not been empirically proven.^{27,28}

The genetics and biochemistry of Group II MB are not as well-characterized, largely because none of the methanotrophs shown to make this form of MB are genetically tractable. As such, the role of various genes in Group II MB synthesis has

largely been inferred from studies done in *M. trichosporium* OB3b or hypothesized from simple BLAST comparisons, e.g., it is suspected that *mbnS* encodes for the sulfotransferase required for sulfonation of Group II MBs. The role of *mbnF* is less clear but, based on homology analyses, appears to encode for a flavin monooxygenase and may be involved in heterocyclic ring formation. ²⁹ There are also two genes of unknown function in the *mbn* gene cluster of *Methyocystis* sp. strain SB2 between *mbnP* and *mbnI* (Figure 2B).

There is a great deal of interest in better understanding the genetics underlying the production of Group II MBs, particularly MB-SB2. That is, it has been shown that MB-SB2 is singularly effective in treating Wilson's disease in animal models and may even be superior to current treatments approved by the US Food and Drug Administration (FDA) for Wilson's disease.³⁰ Briefly, Wilson's disease is a congenital defect where the body cannot tolerate excess amounts of copper due to the dysfunction/mutation of a specific ATPase responsible for removing excess copper in the liver to the bile.^{31,32} Without this active removal strategy, copper accumulates in the liver, leading to the formation of reactive oxidative species that can lead to irreversible liver damage and, if not identified in time, complete liver failure.^{33,34} Current FDA-approved treatments for Wilson's disease (i.e., D-penicill-

amine and trientine) only inhibit further copper collection in the liver and do not remove copper from the liver. As such, current strategies to treat Wilson's disease serve to limit continued disease progression and do not repair any damage that occurred prior to treatment. Further, FDA-approved treatments remove copper via the urine and not the preferred physiological route of the bile. As a result, FDA-approved treatments can lead to redistribution of copper throughout the body, causing copper to accumulate in other organs.^{35–37} In any event, it should be stressed that these treatments are of no use if acute liver damage has already occurred and, in some patients, simply do not work. In such situations, liver failure is likely, and death is almost certain unless a liver transplant is immediately performed, which, although effective in treating Wilson's disease, also imposes significant health risks.^{38–41} Clearly, more effective therapies are urgently needed to treat Wilson's disease.

In rodent studies, MB-SB2 was found to not only prevent copper buildup in the liver but also safely and rapidly deplete excess liver copper from Wilson's disease rats via biliary excretion.³⁰ As such, MB-SB2 is a promising alternative to improving the quality of life of Wilson's disease patients. To realize the significant promise of using MB-SB2 for the treatment of Wilson's disease, mass production of MB-SB2 is necessary for expanded clinical trials. Natural MB production, however, is low, typically on the order of 10-100 mg/L.⁴² Moreover, the production of MB-SB2 currently requires the use of methane as a carbon source, as Methylocystis sp. strain SB2 cannot grow on alternative carbon sources, such as methanol or glucose. Given that methane is explosive in air at concentrations between 5 and 15% (v/v), it can be difficult to scale-up MB production due to safety concerns. Finally, as noted earlier, there is no working genetic system for Methylocystis sp. strain SB2, making it impossible to enhance MB-SB2 production through overexpression of mbn genes in this microorganism. As such, using Methylocystis sp. strain SB2 for mass production of MB-SB2 has significant challenges, and alternative approaches need to be developed.

One possible strategy for improved MB-SB2 production would be to heterologously express genes necessary for MB-SB2 in an alternative methanotroph that is genetically tractable and able to grow on a carbon source other than methane. *M. trichosporium* OB3b is an ideal candidate as it meets both criteria, i.e., it is relatively easy to genetically manipulate, 6,15–18,43 and it can grow on methanol as well as methane. Here, we report on the development and optimization of a heterologous expression system for MB-SB2 production in *M. trichosporium* OB3b.

RESULTS AND DISCUSSION

Bioinformatic Analysis of the *mbn* Gene Cluster of *Methylocystis* sp. Strain SB2. Bioinformatic analyses of the *mbn* gene cluster *Methylocystis* sp. strain SB2 identified three strong promoters upstream of *mbnI*, *mbnP*, and *mbnH* (Figure S1). A ribosome binding site (RBS) was detected for each gene of the *mbn* gene cluster, and the predicted translation rate of *mbnI*, *mbnA*, and *mbnP* was significantly higher (10- to 750-fold) than other genes of the putative methanobactin gene cluster of *Methylocystis* sp. strain SB2 (Figure S2). Collectively, these data suggest that all of these genes, including the unknown genes, may play important roles in the MB-SB2 biosynthesis.

Knock-In and Expression of mbnAS of Methylocystis sp. Strain SB2 in M. trichosporium OB3b \(\Delta mbnAN \) and **AmmoD.** To investigate if MB-SB2 can be heterologously synthesized in M. trichosporium OB3b, we first inserted the gene cluster as shown in Figure S3, i.e., the two genes of unknown function and mbnABCMFS of Methylocystis sp. strain SB2 (hereafter termed mbnAS) into the chromosome of two strains of M. trichosporium OB3b—one where native mbn genes of M. trichosporium OB3b were removed (mbnABCMN, or $\Delta mbnAN::mbnAS$), and another where mmoD, earlier found to play a key role in repressing mbn gene expression, 43 was also removed ($\Delta mmoD$ $\Delta mbnAN::mbnAS$). The presence of mbnAS from Methylocystis sp. strain SB2 as well as the absence of native mbn genes and the plasmid backbone in the chromosome of these two strains were verified by polymerase chain reaction (PCR, Figure S4). The absence of the plasmid in the chromosomes of the two strains was further confirmed by their sensitivity to kanamycin (data not shown). Transcriptional analysis showed that all knocked-in genes were expressed in both M. trichosporium OB3b \(\Delta mbnAN::mbnAS \) and \(\Delta mmoD \) ΔmbnAN::mbnAS (Figure S5). However, UV-vis measurement of the supernatant of these strains actively growing on methane suggests that any MB produced was in a low quantity and incomplete. That is, only a small absorption peak at 386 nm was observed for either strain, suggesting that the Nterminal imidazolone ring of MB-SB2 was present but in low amounts. There was no evidence of any absorption peak at 338 nm, indicating the C-terminal oxazolone ring of MB-SB2 was not formed (Figure S6). Further efforts to purify MB from either strain were unsuccessful (data not shown).

Expression of mbnPH of Methylocystis sp. Strain SB2 in AmbnAN::mbnAS and AmmoD AmbnAN::mbnAS and Their MB-SB2 Production. As little MB-SB2 was found to be produced when mbnAS were expressed heterologously in mutants of M. trichosporium OB3b unable to produce MB-OB3b, we speculated that additional gene(s) is(are) needed, i.e., mbnPH. Initially, we presumed that these genes, although commonly found adjacent to genes critical for MB biosynthesis, were not needed for two reasons: (1) it has been widely assumed that these genes have no role in MB biosynthesis, and (2) the native mbnPH genes of M. trichosporium OB3b are not removed and are very similar to mbnPH of Methylocystis sp. strain SB2 (E values of 10⁻⁷⁷ and 10⁻¹⁶⁷ for mbnP and mbnH, respectively). Further investigation, however, suggested that these genes may be important, as in silico analyses predict that the promoter for mbnPH of Methylocystis sp. strain SB2 is particularly strong (Figure S1), as well as mbnP having a high translation rate (Figure S2). To consider this, we constructed a plasmid based on pTJS-140⁴⁵ with mbnPH inserted and transferred this to M. trichosporium OB3b \(\Delta mbnAN::mbnAS \) and $\Delta mmoD$ $\Delta mbnAN::mbnAS$ for expression of Methylocystis sp. strain SB2 mbnPH. The presence of mbnP in $\Delta mbnAN::mbnAS + pTJS-mbnPH$ and $\Delta mmoD \Delta mbnAN::mb$ nAS + pTJS-mbnPH was verified by PCR (Figure S7). Moreover, the sequence of the inserted mbnAS (together with the inside and outside arm regions, Figure S8) and mbnPH in $\Delta mmoD$ $\Delta mbnAN::mbnAS + pTJS-mbnPH$ was 100% identical to the corresponding/original sequence in *M*. trichosporium OB3b and Methylocystis sp. strain SB2 (Supplemental Data Sets 1 and 2 in the Supporting Information). Transcriptional analysis also showed that mbnPH were expressed in both Δ mbnAN::mbnAS + pTJS-

mbnPH and $\Delta mmoD$ $\Delta mbnAN::mbnAS + pTJS-mbnPH$ (Figure S9).

More importantly, UV—vis absorption spectrophotometry of the spent medium of these constructs clearly showed evidence of MB-SB2 production (Figure 3), i.e., characteristic peaks at

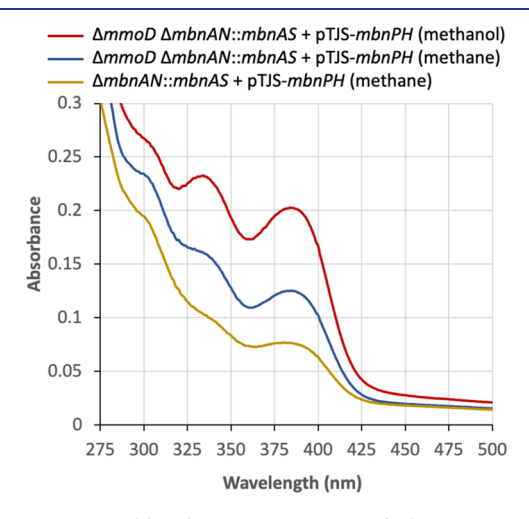


Figure 3. UV—visible absorption spectra of the supernatant of $\Delta mbnAN::mbnAS + pTJS-mbnPH$ and $\Delta mmoD$ $\Delta mbnAN::mbnAS + pTJS-mbnPH$ grown with methane or methanol.

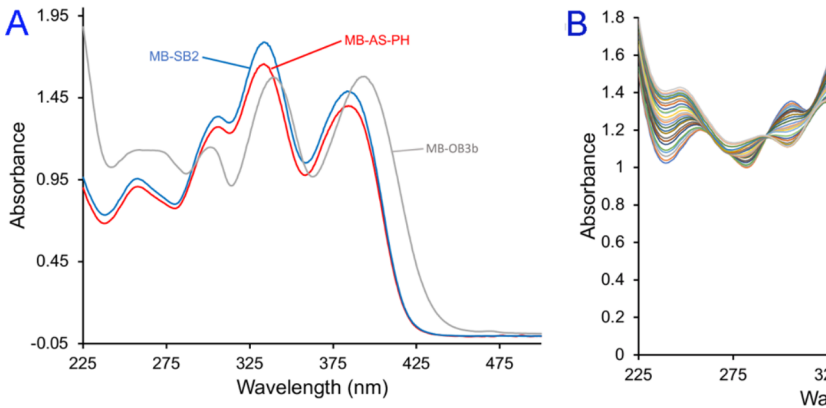
wavelengths of 303, 336, and 386 nm (the latter two are associated with the oxazolone and imidazole rings of MB-SB2, respectively). Overall, absorption was higher in the supernatant of $\Delta mmoD$ $\Delta mbnAN + mbnAS + pTJS-mbnPH$ than in $\Delta mbnAN::mbnAS + pTJS-mbnPH$, indicating higher MB-SB2 production in $\Delta mmoD$ $\Delta mbnAN::mbnAS + pTJS-mbnPH$. We therefore selected this construct for further investigation. Moreover, it was found that $\Delta mmoD$ $\Delta mbnAN::mbnAS + pTJS-mbnPH$ could also grow with methanol and that MB-SB2 production in this strain was significantly higher when methanol was used as the growth substrate as compared to methane-grown cultures (Figure 3).

Verification of Heterologous Production of MB-SB2. To confirm that MB-SB2 was heterologously produced using *M. trichosporium* OB3b as a production platform, the $\Delta mmoD$ $\Delta mbnAN::mbnAS + pTJS-mbnPH$ construct was grown in a 10 L fermenter, and MB was purified from the spent medium.

Comparison of the UV–visible absorption spectra of MB from $\Delta mmoD$ $\Delta mbnAN::mbnAS$ + pTJS-mbnPH to that of verified MB-OB3b and MB-SB2 standards clearly shows that the MB made by this production construct closely resembles that of MB-SB2 (Figure 4A). In addition, copper titration assays show the same pattern of absorption maxima decrease with increasing copper, as well as a slight blue shift of the peak at 338 nm (diagnostic for a C-terminal oxazolone ring) to 326 nm as observed before for MB-SB2^{46,47} (Figure 4B).

In addition to copper titration assays, the purified MB from $\Delta mmoD$ $\Delta mbnAN::mbnAS + pTJS-mbnPH$ was subjected to acid digestion. That is, it was shown earlier that the oxazolone rings of MB are particularly susceptible to acid-catalyzed hydrolysis 46,47 while the N-terminal imidazolone ring of MB-SB2 is very resistant to such degradation. Indeed, digestion of MB from $\Delta mmoD$ $\Delta mbnAN::mbnAS + pTJS-mbnPH$ in 100 µM acetic acid over 10 h clearly shows complete loss of the Cterminal oxazolone ring as indicated by the loss of the absorption peak at 338 nm. The absorption peak at 387 nm, however, showed little decrease, and thus, it is indicative that this peak is indeed not due to an oxazolone ring but rather results from the N-terminal ring being an imidazolone moiety (Figure 5). Furthermore, the UV-visible absorption spectra of the MB from $\Delta mmoD$ $\Delta mbnAN::mbnAS + pTJS-mbnPH$ following hydrolysis of the oxazolone group was identical to that observed following hydrolysis of the oxazolone group in MB-SB2 (Figure 5B).4

Mass Spectrometry of MB-SB2 With and Without **Copper.** Metal-free MB-SB2 produced by M. trichosporium OB3b $\Delta mmoD \Delta mbnAN::mbnAS + pTJS-mbnPH$ showed a molecular mass of 851.2115 (Figure 6), which was very similar to what was originally purified from Methylocystis sp. strain SB2 in 2010 (851.1997). 46 Upon the addition of copper, MB from $\Delta mmoD \ \Delta mbnAN::mbnAS + pTJS-mbnPH$ bound one copper ion (again as found earlier 46) with a molecular mass of 913.1353 (Figure 6). Loss of one proton following Cu²⁺ binding and reduction to Cu⁺ was also consistent with previous studies on the MB from Methylocystis sp. strain SB2.⁴⁸ We would like to note that there is some variability in measuring the mass of methanobactins, e.g., when repeating liquid chromatography-mass spectroscopy (LC-MS) analyses of MB-SB2 produced by M. trichosporium OB3b ΔmmoD $\Delta mbnAN::mbnAS + pTJS-mbnPH$, a mass of 851.1934 was determined in this second measurement of the same sample,



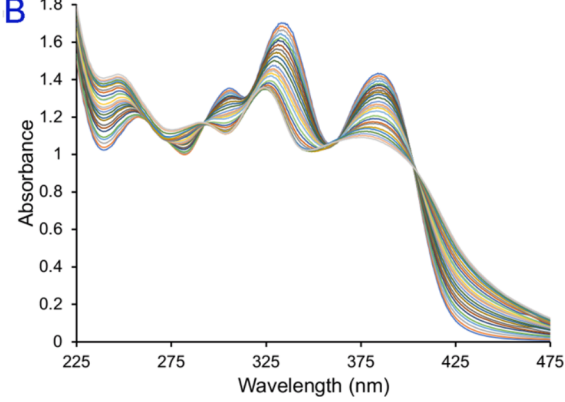


Figure 4. (A) UV-visible absorption spectra of 75 μ M MB-SB2 from M. trichosporium OB3b Δ mmoD Δ mbnAN::mbnAS + pTJS-mbnPH (MB-AS + PH; red trace), 75 μ M MB-SB2 (blue trace), and 100 μ M MB-OB3b. (B) UV-visible absorption spectra of 75 μ M M. trichosporium OB3b Δ mmoD Δ mbnAN::mbnAS + pTJS-mbnPH as isolated and following 24 0.05 molar additions of CuCl₂.

ACS Synthetic Biology pubs.acs.org/synthbio Research Article

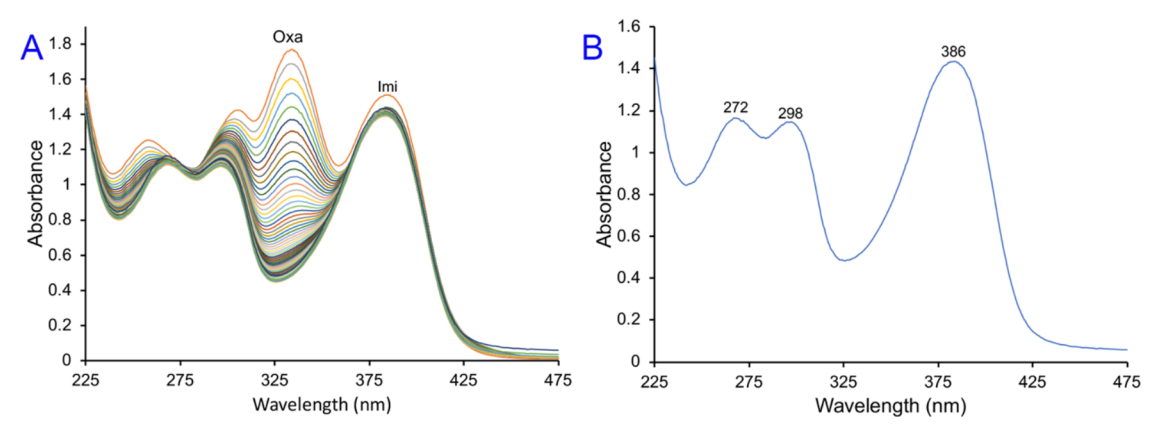


Figure 5. (A) UV-visible absorption spectra of 75 μ M MB-SB2 from M. trichosporium OB3b Δ mmoD Δ mbnAN::mbnAS + pTJS-mbnPH in 100 μ M acetic acid and scanned every 20 min for 10 h at 25 °C. (B) UV-visible absorption spectra of 75 μ M MB-SB2 from M. trichosporium OB3b Δ mmoD Δ mbnAN::mbnAS + pTJS-mbnPH following exposure to 100 μ M acidic acid for 10 h at 25 °C.

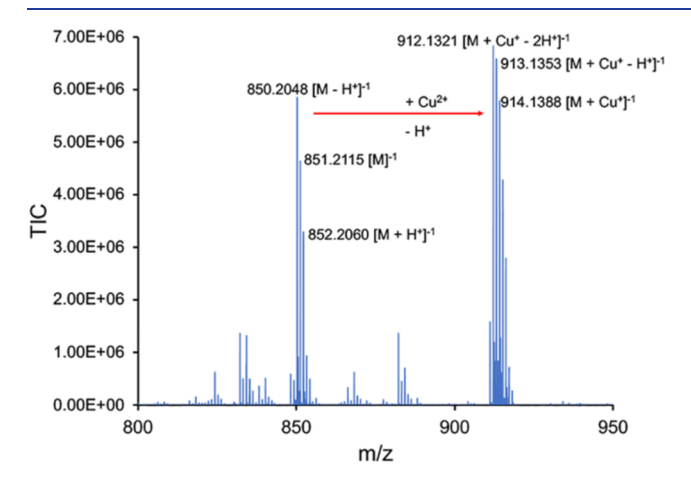


Figure 6. Mass spectrum in negative ion mode of MB as isolated from M. trichosporium OB3b $\Delta mmoD$ $\Delta mbnAN::mbnAS + pTJS-mbnPH$ and following the addition of 0.6 μ mole CuCl₂ per μ mole of MB from M. trichosporium OB3b $\Delta mmoD$ $\Delta mbnAN::mbnAS + pTJS-mbnPH$.

while the mass for validated MB-SB2 was found to be 851.1887 when analyzed as part of work presented here (i.e., slightly less than 851.1997 as reported earlier; ⁴⁶ Figure S10).

Nuclear Magnetic Resonance (NMR) Spectroscopy of MB from M. trichosporium OB3b Δ mmoD Δ mbnAN::mb**nAS** + **pTJS-mbnPH.** Finally, to confirm that M. trichosporium OB3b $\Delta mmoD \Delta mbnAN::mbnAS + pTJS-mbnPH$ was indeed producing MB-SB2, ¹H-spectra of the purified compound associated with copper was collected and compared to that identified in the original description of MB-SB2 by Krentz et al. 46 It should be noted that the ¹H spectrum collected for MB with copper bound as metal-free MB has multiple conformations, making structural studies of MBs via solution NMR challenging. However, the addition of copper stabilizes MB into one conformation, allowing for effective NMR analyses. As can be seen in Figure 7, MB from M. trichosporium OB3b $\Delta mmoD \Delta mbnAN::mbnAS + pTJS-mbnPH$ is identical to that presented in the initial characterization of MB-SB2, further supporting the conclusion that MB-SB2 was indeed heterologously synthesized using our expression platform.

This result is significant for several reasons, perhaps most importantly, as it provides an alternative strategy for the production of MB-SB2 to facilitate its use in human clinical trials for the treatment of Wilson's disease. That is, although

methane is an inexpensive carbon source, its use for the production of secondary metabolites (such as MB-SB2) is problematic given that yields of MB in wildtype methanotrophs are low, methane/air mixtures can be explosive, and overall microbial growth can be limited by mass transfer of methane into solution. Herein, we show that not only we can heterologously produce MB-SB2 with methane as the growth substrate in a mutant of M. trichosporium OB3b where native mbn genes and mmoD were deleted, but we can also do so using methanol. This finding is especially exciting as methanol, although more expensive than natural gas, is actually cheaper than chemically pure methane, which is commonly used for methanotrophic growth. That is, the cost of high-performance liquid chromatography (HPLC) grade (99.9%) methanol as used here is ~ 5 ¢/g, while natural gas (85–90% methane with impurities that can inhibit methanotrophy) is $\sim 0.03 \, \text{¢/g}$ and the cost of chemically pure (99.5%) methane is $\sim 20-50$ ¢/g (prices derived from a web search of methane/methanol prices as of March 15, 2024). Further, methanol can be much more easily added than methane, and indeed, MB-SB2 yields were greater on methanol than on methane in this mutant. Although we showed earlier that mmoD represses native MB synthesis in M. trichosporium OB3b when grown on methane, 43 production of MB by this strain with methanol as the growth substrate was unexpected, as previous efforts in our laboratories to produce native MB in M. trichosporium OB3b when grown on methanol have never been successful (data not shown). Clearly, mmoD plays a critical regulatory role in M. trichosporium OB3b, and it is strongly recommended that greater effort be put forward to fully delineate not only the range of such regulation but also the mechanism(s) by which such control is exerted by mmoD.

In addition to identifying a key regulatory element controlling the production of MB, we also show that *mbnPH* is critical for the biosynthesis of MB-SB2. Such a finding contradicts earlier speculation that the products of these genes served to remove copper from MB after copper-MB complexes are reinternalized.^{27,28} At this time, we do not know what the exact role(s) of MbnPH may be, but it may be involved in oxazolone ring synthesis given that these genes are found in both Group I and II MB gene clusters, or it may have a role in removing the leader peptide from MB. We hasten to stress, however, that these statements are speculative and provide them to induce broader discussion and investigation into these intriguing genes and their products.

ACS Synthetic Biology pubs.acs.org/synthbio Research Article

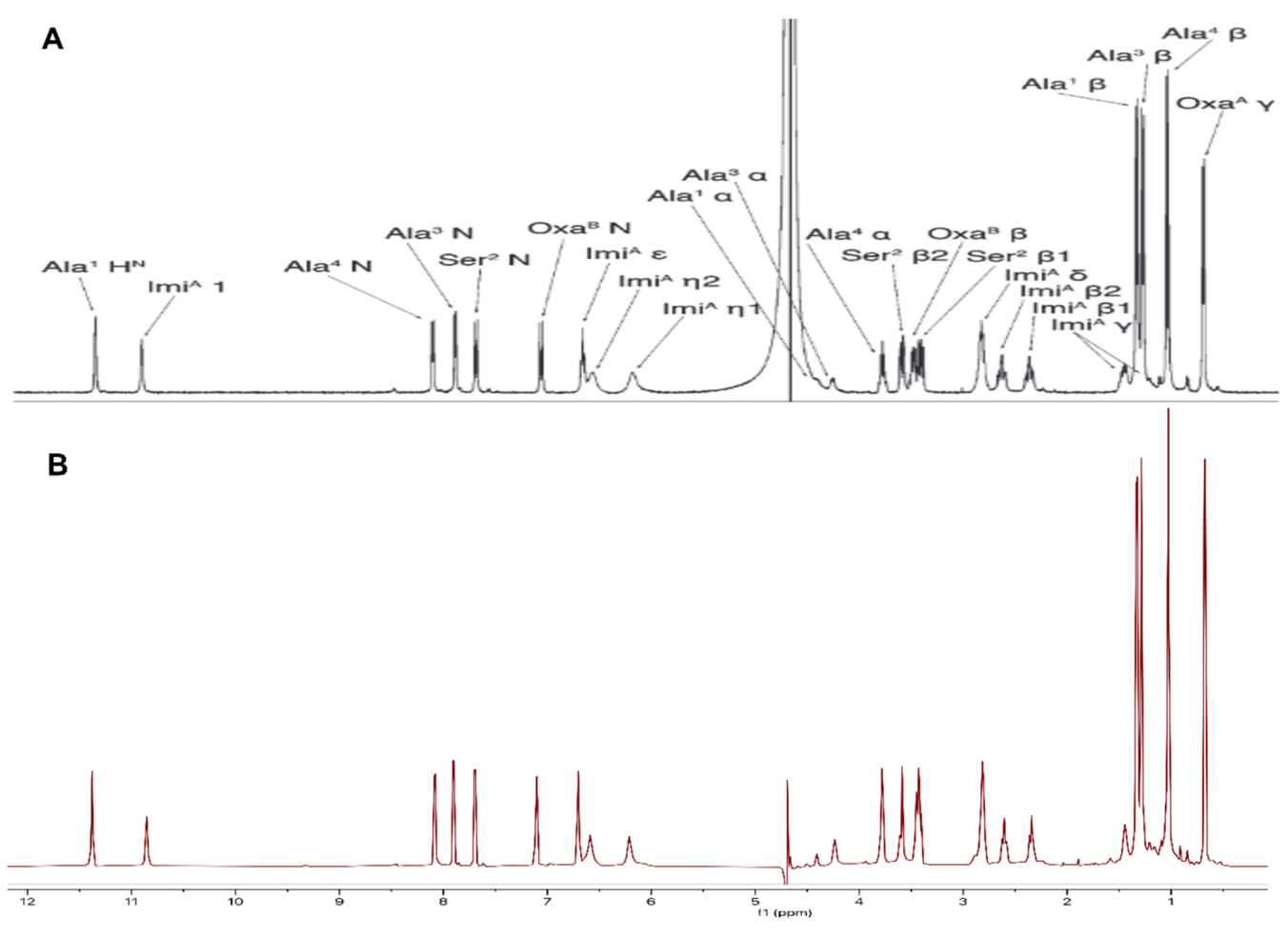


Figure 7. ¹H spectrum of Cu-MB from (A) Methylocystis species strain SB2 as reported by Krentz et al. ⁴⁶ and (B) M. trichosporium OB3b Δ mmoD Δ mbnAN::mbnAS + pTJS-mbnPH. Note that panel (A) is reprinted with permission from Krentz et al., Biochemistry, 49:10117–10130, 2010.

Finally, by showing that MB-SB2 can be heterologously produced using M. trichosporium OB3b as a production platform, we now have significant opportunities to achieve hitherto unobtainable goals. First, we can experimentally verify the function of unique Group II mbn genes, i.e., mbnF and mbnS, through the construction of mutants wherein these genes are removed, either singly or in combination, and then characterize the structure of MB-SB2 produced using our production platform. Second, this approach also provides us with the ability to generate modified forms of MB-SB2, e.g., it may be possible to delete several codons encoding for Cterminal amino acids and/or amino acids between the two heterocyclic rings to reduce the size of MB-SB2. Pursuing these objectives may increase the range of copper-related diseases that can be treated by MB, e.g., by reducing the size of MB-SB2, it may be possible for it to cross the blood-brain barrier and thus remove copper from the brain. That is, Wilson's disease can also lead to a suite of neurological problems due to the accumulation of copper in the brain, including tremors, seizures, dystonia, and parkinsonism. 49 In addition, although the causative agent(s) of late-onset Alzheimer's disease is(are) not defined, copper appears to play a key role. 50-60 Thus, the findings here create a panoply of both basic and applied research opportunities that we encourage the field to consider.

MATERIALS AND METHODS

Growth Conditions. Wildtype *M. trichosporium* OB3b and various mutants (Table 1) were grown in a nitrate mineral salt

Table 1. M. trichosporium OB3b Mutant Strains Used in This Study

strain	description	refs
$\Delta mbnAN$	M. trichosporium OB3b with mbnAN deleted	15
$\Delta mmoD$	M. trichosporium OB3b with mmoD deleted	43
ΔmbnAN::mbnAS	ΔmbnAN with mbnAS of Methylocystis sp. strain SB2 knocked in its genome	this study
$\Delta mmoD$ $\Delta mbnAN::mbnAS$	ΔmmoD with mbnAS of Methylocystis sp. strain SB2 knocked in its genome and replaced its original mbnAN	this study
$\Delta mbnAN::mbnAS + pTJS-mbnPH$	ΔmbnAN::mbnAS carrying pTJS-140 with mbnPH of Methylocystis sp. strain SB2	this study
$\Delta mmoD$ $\Delta mbnAN::mbnAS$ + pTJS- $mbnPH$	ΔmmoD ΔmbnAN-mbnAS carrying pTJS- 140 with mbnPH of Methylocystis sp. strain SB2	this study

(NMS) medium 61 with or without 25 $\mu g/mL$ kanamycin and in the absence (no added) or presence of copper (0.2 or 1 μM as CuCl₂). Methane and air were added at a methane-to-air ratio of 1:2. Cultures were incubated in the dark at 30 °C. When methanol was used as the carbon source, HPLC plus grade methanol was added to the NMS medium at a concentration of 0.25%. Liquid cultures were grown in 250

mL side arm Erlenmeyer flasks with 20 mL of NMS medium with shaking at 200 rpm. Growth was monitored by measuring the optical density at 600 nm (OD₆₀₀) with a Genesys 20 visible spectrophotometer (Spectronic Unicam, Waltham, MA). Triplicate biological cultures were prepared under all experimental conditions. Cultures were harvested at the middle-to-late exponential phase (OD₆₀₀ of ~0.75) for RNA isolation and transcriptional analysis of specific gene expression. *E. coli* was grown in Luria—Bertani broth (LB) at 37 °C with or without a supplement of 25 μ g/mL kanamycin.

mbn Gene Cluster of Methylocystis sp. Strain SB2 Analysis. Promoter and ribosome binding site (RBS) strengths were predicted using the Promoter Calculator⁶² and RBS Calculator, respectively, with the default parameters.⁶³

Knock-In of Methylocystis sp. Strain SB2 mbn Genes into M. trichosporium OB3b. mbnAS plus the two unknown genes were first knocked in a previous mutant of M. trichosporium OB3b where the native mbn genes, mbnABCMN, were removed using a sucrose counter-selection protocol (M. trichosporium OB3b \(\Delta mbnAN \). 64 Briefly, the presumed methanobactin gene cluster, mbnABCMFS, plus the two unknown genes (hereafter labeled mbnAS) of Methylocystis sp. strain SB2, and the upstream and downstream regions (arms) of mbnAN of M. trichosporium OB3b were PCRamplified using the primers listed in Table S1 (specific genes removed/added are shown in Figure S3). The arms and mbnAS were digested with the appropriate restriction enzymes, ligated together, and subsequently inserted into the pK18mobsacB mobilizable suicide vector. 65 pK18mobsacB vector with mbnAS and arms was transferred to E. coli Top10 for production (Invitrogen, Carlsbad, CA). The plasmid was then extracted from transformed E. coli Top10 using the Plasmid Mini Kit (Qiagen, Hilden, Germany) following the manufacturer's instructions and then sent to Eurofins for Whole Plasmid Sequencing to confirm the accuracy of the PCR and cloning. After sequence conformation, the plasmid was then transformed to E. coli S17-1⁶⁶ for conjugation. Conjugation of E. coli S17-1 carrying the constructed vector with M. trichosporium OB3b AmbnAN was performed as described by Martin and Murrell.⁶⁷ Transconjugants were grown on NMS plates supplemented with 25 µg/mL kanamycin and 10 μ g/mL nalidixic acid. The generated kanamycin-resistant transconjugant colonies (after 10 days of incubation) were transferred to NMS plates with kanamycin, incubated for 7 days, and subsequently transferred to NMS plates with 2.5% sucrose (mass/vol). Sucrose-resistant colonies were generated after 10 days of incubation and were screened for knock-in of mbnAS by colony PCR. Successful mbnAS knock-in mutants were further confirmed by PCR with DNA extracted from the mutant using the DNeasy PowerSoil Pro Kit (Qiagen, Hilden, Germany) following manufacturer's instructions.

In addition to knocking in mbnAS in M. trichosporium OB3b $\Delta mbnAN$, we also constructed a second production platform where mmoD, a gene in the mmo operon—encoding for the soluble methane monooxygenase, was also removed to create M. trichosporium OB3b $\Delta mmoD$ $\Delta mbnAN::mbnAS$. This mutant was constructed as we have shown earlier that MmoD serves to repress MB-OB3b biosynthesis, 43 and we speculated that it may also repress heterologous expression of mbnAS of Methylocystis sp. strain SB2 in M. trichosporium OB3b. Briefly, the E. coli S17—1 carrying pK18mobsacB with

mbnAS and arms was conjugated with M. trichosporium OB3b $\Delta mmoD$. Transconjugants growth and selection of the marker exchange mutant ($\Delta mmoD$ $\Delta mbnAN::mbnAS$) were performed as described above. We should stress that all strains constructed where genes were either knocked-out or knocked-in the chromosome of M. trichosporium OB3b were done so using markerless rearrangements.

Heterologous Expression of mbnPH of Methylocystis sp. Strain SB2 in Δ mbnAN::mbnAS and Δ mmmoD Δ mbnAN::mbnAS. mbnPH from Methylocystis sp. strain SB2 was amplified by PCR using the primers listed in Table S1. mbnPH was cloned into pTJS140 broad-host-range cloning vector (predigested with KpnI restriction enzyme)⁴⁵ using NEBuilder HiFi DNA Assembly Cloning Kit. The pTJS140 vector with mbnPH (pTJS-mbnPH) was transformed to E. coli S17–1 as described above. E. coli S17–1 with the constructed plasmid was conjugated with Δ mmoD Δ mbnAN::mbnAS. Transconjugants were grown on NMS plates supplemented with 25 μ g/mL kanamycin and 10 μ g/mL nalidixic acid. Selection and conformation of Δ mmoD Δ mbnAN::mbnAS with pTJS-mbnPH were done as described above.

Sequencing of mbnAS and mbnPH in \(\Delta\text{mmmoD}\) \(\Delta\text{mbnAS}\): mbnAS with pTJS-mbnPH. To verify that mbnAS was knocked in the correct position of the chromosome (i.e., in place of native mbn genes), we designed a primer set targeting the expected mbnAS knock-in region outside the arms (Table S1, Figure S4). The PCR product was cloned into pK18mobsacB vector (predigested with HindIII restriction enzyme) using NEBuilder HiFi DNA Assembly Cloning Kit and then transformed to E. coli 5-alpha (NEB). The plasmid with the PCR product of mbnAS was extracted from E. coli 5-alpha and sent to Eurofins for Whole Plasmid Sequencing. mbnPH was PCR-amplified using the mbnPH primers listed in Table S1 (PCR region as shown in Figure S8). The PCR product was purified and sent to Eurofins for Sanger Sequencing.

RNA Isolation and Reverse Transcription PCR (RT-PCR). RNA isolation was performed with a bead-beating procedure followed by column purification using an RNeasy Mini Kit (Qiagen, Hilden, Germany) as described before. Genomic DNA was removed from the column with RNase-free DNase (Qiagen, Hilden, Germany) treatment. Absence of genomic DNA was confirmed by *mbnA* genes (*Methylocystis* sp. strain SB2, Figure 2B) targeted PCR with extracted RNA samples as templates. Purified RNA was quantified using a NanoDrop 1000 Spectrophotometer (Thermo Scientific, Wilmington, DE). cDNA was synthesized from 200 ng total RNA using SuperScript III Reverse Transcriptase (Invitrogen, Carlsbad, CA) following manufacturer's instructions.

RT-PCR was performed to verify the expression of the knocked-in *mbn* genes of *Methylocystis* sp. strain SB2 in the mutants ($\Delta mbnAN::mbnAS$, $\Delta mmmoD$ $\Delta mbnAN::mbnAS$, and $\Delta mmmoD$ $\Delta mbnAN::mbnAS$ with pTJS-mbnPH). Primers for RT-PCR were designed using the NCBI online primer design tool (http://www.ncbi.nlm.nih.gov/tools/primer-blast/). Primer specificity was checked with the online tool and further verified by PCR (using genomic DNAs from *Methylocystis* sp. strain SB2 and *M. trichosporium* OB3b as the templates) and sequencing. RT-PCR was performed with 1 μ L of cDNA and the following program: 95 °C for 5 min, followed by 30 cycles of 95 °C for 30 s, 55 °C for 30 s, and 72 °C for 30 s, and final extension at 72 °C for 5 min.

Isolation of Methanobactins. *Methylocystis* sp. strain SB2 and *M. trichosporium* OB3b were cultured, and the methanobactins from each strain were isolated as previously described. M. trichosporium $\Delta mmoD$ $\Delta mbnAN::mbnAS + pTJS-mbnPH$ was cultured in nitrate mineral salt medium with kanamycin but no amended copper and isolated as described above.

Liquid Chromatography–Mass Spectroscopy (LC-MS). Mass was determined on a Waters SYNAPT G2-Si High Definition Mass Spectrometer coupled to a Waters H-Class UHPLC system. The peptide (10 μ L injection at 2 mg/mL) was isolated using a Restek C4 5 μ m 50 mm × 1 mm column at a flow rate of 400 μ L/min with a linear gradient from 5–100% acetonitrile/water (both containing 0.1% formic acid). The peptide was introduced to SYNAPT G2-Si using a dual orthogonal API source (LockSpray ESI/APCI). The mass spectrometer was operated in ESI negative resolution mode in the range of 50–5000 Da. The capillary voltage was set to 2.5 kV with a sampling cone voltage of 40 V, a source temperature of 100 °C, and a desolvation temperature of 250 °C. The cone gas was set to 50 L/h with desolvation gas at 600 L/h, and the nebulizer was set to 6.5 bar.

NMR Spectroscopy. A nuclear magnetic resonance (NMR) experiment was conducted at the BioNMR Core facility at the University of Michigan. The NMR experiment was conducted on an 800 MHz Bruker NMR spectrometer equipped with a 5 mm Triple resonance inverse detection TCI cryoprobe with automatic tuning and matching. Metal-free MB was dissolved in 10 mM phosphate buffer (pH 6.5) with 10% D $_2$ O to a concentration of 3 mM. CuSO $_4$ was then added to the MB solution to achieve a final Cu/MB molar ratio of 0.9:1. After CuSO $_4$ was added, the pH of the MB solution was readjusted to 6.5 with NaOH. NMR analyses were conducted at 5 °C. The MB solution was placed in a NE-SL5-7 NMR tube (New Era Enterprises, Inc., Vineland, NJ). The NMR spectra were analyzed using MestreNova software.

Other Methods. UV—visible absorption spectroscopy, copper titrations, and acid hydrolysis were determined as previously described.⁴⁷

ASSOCIATED CONTENT

Solution Supporting Information

The Supporting Information is available free of charge at https://pubs.acs.org/doi/10.1021/acssynbio.4c00026.

Additional experimental details (e.g., primer sets used, overview of mutant construction) and supplementary data (ribosomal binding site translation rates, validation of mutants via selective PCR, and additional spectral data) (PDF)

AUTHOR INFORMATION

Corresponding Author

Jeremy D. Semrau — Department of Civil and Environmental Engineering, University of Michigan, Ann Arbor, Michigan 48109-2125, United States; orcid.org/0000-0002-1670-9984; Phone: 734-764-6487; Email: jsemrau@umich.edu

Authors

Peng Peng — Department of Civil and Environmental Engineering, University of Michigan, Ann Arbor, Michigan 48109-2125, United States; orcid.org/0000-0001-9982-5210 Alan A. DiSpirito — Roy J. Carver Department of Biochemistry, Biophysics and Molecular Biology, Iowa State University, Ames, Iowa 50011-3260, United States

Braden J. Lewis — Roy J. Carver Department of Biochemistry, Biophysics and Molecular Biology, Iowa State University, Ames, Iowa 50011-3260, United States

Joel D. Nott – Office of Biotechnology Protein Facility, Iowa State University, Ames, Iowa 50011-3260, United States

Complete contact information is available at: https://pubs.acs.org/10.1021/acssynbio.4c00026

Author Contributions

J.D.S. and A.A.D. conceived of experiments, data analyses, writing, and were responsible for project administration and funding. P.P. was primarily responsible for experimental design, data collection, and writing. B.J.L. assisted in cultivation of methanotrophs, isolation of methanobactins, and spectral analysis. J.D.N. was primarily responsible for molecular mass determinations of methanobactins.

Notes

The authors declare the following competing financial interest(s): JDS and AAD are co-inventors in a patent for the use of methanobactin in the treatment of Wilsons disease (US Patent #11,000,568) that has been licensed to ArborMed. JDS and AAD also hold a patent on methanobactin from Methylocystis strain SB2 (US Patent # 8,629,239). JDS, AAD, and PP also have applied for a patent for the heterologous expression of MB.

ACKNOWLEDGMENTS

This research was supported by the U.S. Department of Energy Office of Science (Grant #DE-SC0020174 to J.D.S. and A.A.D.) and the U.S. National Science Foundation (Grant #1912482 to J.D.S.). The authors thank Debashish Sahu, Director of the Biomolecular NMR Research Laboratory at the University of Michigan for invaluable assistance in performing ¹H NMR analyses.

ABBREVIATIONS

MB:methanobactin

MB-SB2:methanobactin from *Methylocystis* sp. strain SB2 MB-OB3b:methanobactin from *Methylosinus trichosporium* OB3b

 $\Delta mmoD$:markerless deletion of mmoD in M. trichosporium OB3b

 $\Delta mbnAN$:markerless removal of mbnABCMN in M. trichosporium OB3b

 $\Delta mmoD$ $\Delta mbnAN::mbnAS:$ markerless insertion of mbnABCMFS of Methylocystis sp. strain SB2 into the chromosome of Methylosinus trichosporium OB3b

pTJS-mbnPH:plasmid pTJS-140 with mbnPH of Methylocystis sp. strain SB2

REFERENCES

- (1) DiSpirito, A. A.; Semrau, J. D.; Murrell, J. C.; Gallagher, W. H.; Dennison, C.; Vuilleumier, S. Methanobactin and the link between copper and bacterial methane oxidation. *Microbiol. Mol. Biol. Rev.* **2016**, *80* (2), 387–409.
- (2) Kenney, G. E.; Rosenzweig, A. C. Chalkophores. *Annu. Rev. Biochem.* **2018**, 87, 645–676.
- (3) Choi, D. W.; Zea, C. J.; Do, Y. S.; Semrau, J. D.; Antholine, W. E.; Hargrove, M. S.; Pohl, N. L.; Boyd, E. S.; Geesey, G. G.; Hartsel, S. C.; et al. Spectral, kinetic, and thermodynamic properties of Cu (I)

- and Cu (II) binding by methanobactin from Methylosinus trichosporium OB3b. Biochemistry 2006, 45 (5), 1442-1453.
- (4) Kim, H. J.; Graham, D. W.; DiSpirito, A. A.; Alterman, M. A.; Galeva, N.; Larive, C. K.; Asunskis, D.; Sherwood, P. M. Methanobactin, a copper-acquisition compound from methane-oxidizing bacteria. *Science* **2004**, *305* (5690), 1612–1615.
- (5) Semrau, J. D.; DiSpirito, A. A.; Gu, W.; Yoon, S. Metals and methanotrophy. *Appl. Environ. Microbiol.* **2018**, 84 (6), e02289–02217.
- (6) Semrau, J. D.; Jagadevan, S.; DiSpirito, A. A.; Khalifa, A.; Scanlan, J.; Bergman, B. H.; Freemeier, B. C.; Baral, B. S.; Bandow, N. L.; Vorobev, A.; et al. Methanobactin and MmoD work in concert to act as the 'copper-switch' in methanotrophs. *Environ. Microbiol.* **2013**, 15 (11), 3077–3086.
- (7) Choi, D. W.; Do, Y. S.; Zea, C. J.; McEllistrem, M. T.; Lee, S.-W.; Semrau, J. D.; Pohl, N. L.; Kisting, C. J.; Scardino, L. L.; Hartsel, S. C. Spectral and thermodynamic properties of Ag (I), Au (III), Cd (II), Co (II), Fe (III), Hg (II), Mn (II), Ni (II), Pb (II), U (IV), and Zn (II) binding by methanobactin from *Methylosinus trichosporium* OB3b. *J. Inorg. Biochem.* **2006**, *100* (12), 2150–2161.
- (8) El Ghazouani, A.; Baslé, A.; Gray, J.; Graham, D. W.; Firbank, S. J.; Dennison, C. Variations in methanobactin structure influences copper utilization by methane-oxidizing bacteria. *Proc. Natl. Acad. Sci. U.S.A.* **2012**, *109* (22), 8400–8404.
- (9) Chi Fru, E.; Gray, N.; McCann, C.; Baptista, J. d. C.; Christgen, B.; Talbot, H.; Ghazouani, A. E.; Dennison, C.; Graham, D. Effects of copper mineralogy and methanobactin on cell growth and sMMO activity in *Methylosinus trichosporium* OB3b. *Biogeosciences* **2011**, 8 (10), 2887–2894.
- (10) Pesch, M. L.; Hoffmann, M.; Christl, I.; Kraemer, S. M.; Kretzschmar, R. Competitive ligand exchange between Cu-humic acid complexes and methanobactin. *Geobiology* **2013**, *11* (1), 44–54.
- (11) Kulczycki, E.; Fowle, D. A.; Knapp, C.; Graham, D. W.; Roberts, J. A. Methanobactin-promoted dissolution of Cu-substituted borosilicate glass. *Geobiology* **2007**, *5* (3), 251–263.
- (12) Park, Y. J.; Roberts, G. M.; Montaser, R.; Kenney, G. E.; Thomas, P. M.; Kelleher, N. L.; Rosenzweig, A. C. Characterization of a copper-chelating natural product from the methanotroph *Methylosinus* sp. LW3. *Biochemistry* **2021**, *60* (38), 2845–2850.
- (13) Semrau, J. D.; DiSpirito, A. A.; Obulisamy, P. K.; Kang-Yun, C. S. Methanobactin from methanotrophs: genetics, structure, function and potential applications. *FEMS Microbiol. Lett.* **2020**, *367* (5), No. fnaa045.
- (14) El Ghazouani, A.; Basle, A.; Firbank, S. J.; Knapp, C. W.; Gray, J.; Graham, D. W.; Dennison, C. Copper-binding properties and structures of methanobactins from *Methylosinus trichosporium* OB3b. *Inorg. Chem.* **2011**, *50* (4), 1378–1391.
- (15) Gu, W.; Baral, B. S.; DiSpirito, A. A.; Semrau, J. D. An aminotransferase is responsible for the deamination of the N-terminal leucine and required for formation of oxazolone ring A in methanobactin of *Methylosinus trichosporium* OB3b. *Appl. Environ. Microbiol.* 2017, 83 (1), e02619–02616.
- (16) Gu, W.; Haque, M. F. U.; Baral, B. S.; Turpin, E. A.; Bandow, N. L.; Kremmer, E.; Flatley, A.; Zischka, H.; DiSpirito, A. A.; Semrau, J. D. A TonB-dependent transporter is responsible for methanobactin uptake by *Methylosinus trichosporium* OB3b. *Appl. Environ. Microbiol.* **2016**, 82 (6), 1917–1923.
- (17) Peng, P.; Gu, W.; DiSpirito, A. A.; Semrau, J. D. Multiple Mechanisms for Copper Uptake by *Methylosinus trichosporium* OB3b in the Presence of Heterologous Methanobactin. *mBio* **2022**, *13* (5), e02239–02222.
- (18) Peng, P.; Kang-Yun, C. S.; Chang, J.; Gu, W.; DiSpirito, A. A.; Semrau, J. D. Two TonB-dependent transporters in *Methylosinus trichosporium* OB3b are responsible for uptake of different forms of methanobactin and are involved in the canonical 'copper switch'. *Appl. Environ. Microbiol.* **2022**, 88 (1), e01793–01721.
- (19) Dershwitz, P.; Gu, W.; Roche, J.; Kang-Yun, C. S.; Semrau, J. D.; Bobik, T. A.; Fulton, B.; Zischka, H.; DiSpirito, A. A. MbnC Is Not Required for the Formation of the N-Terminal Oxazolone in the

- Methanobactin from Methylosinus trichosporium OB3b. Appl. Environ. Microbiol. 2022, 88 (2), e01841–01821.
- (20) Kenney, G. E.; Dassama, L. M.; Pandelia, M.-E.; Gizzi, A. S.; Martinie, R. J.; Gao, P.; DeHart, C. J.; Schachner, L. F.; Skinner, O. S.; Ro, S. Y.; et al. The biosynthesis of methanobactin. *Science* **2018**, 359 (6382), 1411–1416.
- (21) Bishop, G. R.; Brooks, H. B.; Davidson, V. L. Evidence for a tryptophan tryptophylquinone aminosemiquinone intermediate in the physiologic reaction between methylamine dehydrogenase and amicyanin. *Biochemistry* **1996**, *35* (27), 8948–8954.
- (22) McIntire, W. S.; Wemmer, D. E.; Chistoserdov, A.; Lidstrom, M. E. A new cofactor in a prokaryotic enzyme: tryptophan tryptophylquinone as the redox prosthetic group in methylamine dehydrogenase. *Science* **1991**, 252 (5007), 817–824.
- (23) Davidson, V. L. Pyrroloquinoline quinone (PQQ) from methanol dehydrogenase and tryptophan tryptophylquinone (TTQ) from methylamine dehydrogenase. *Adv. Protein Chem.* **2001**, *58*, 95–140.
- (24) Davidson, V. L. Protein-derived cofactors. Expanding the scope of post-translational modifications. *Biochemistry* **2007**, *46* (18), 5283–5292.
- (25) Wilmot, C. M.; Yukl, E. T. MauG: a di-heme enzyme required for methylamine dehydrogenase maturation. *Dalton Trans.* **2013**, 42 (9), 3127–3135.
- (26) Frato, K. E.; Walsh, K. A.; Elliott, S. J. Functionally distinct bacterial cytochrome c peroxidases proceed through a common (electro) catalytic intermediate. *Biochemistry* **2016**, *55* (1), 125–132.
- (27) Kenney, G. E.; Dassama, L. M.; Manesis, A. C.; Ross, M. O.; Chen, S.; Hoffman, B. M.; Rosenzweig, A. C. MbnH is a diheme MauG-like protein associated with microbial copper homeostasis. *J. Biol. Chem.* **2019**, 294 (44), 16141–16151.
- (28) Dassama, L. M. K.; Kenney, G. E.; Rosenzweig, A. C. Methanobactins: from genome to function. *Metallomics* **2017**, 9 (1), 7–20.
- (29) Stewart, A.; Dershwitz, P.; Stewart, C.; Sawaya, M. R.; Yeates, T. O.; Semrau, J. D.; Zischka, H.; DiSpirito, A. A.; Bobik, T. A. Crystal structure of MbnF: an NADPH-dependent flavin monooxygenase from *Methylocystis* strain SB2. *Acta Crystallogr., Sect. F: Struct. Biol. Commun.* **2023**, 79 (5), 111–118.
- (30) Einer, C.; Munk, D. E.; Park, E.; Akdogan, B.; Nagel, J.; Lichtmannegger, J.; Eberhagen, C.; Rieder, T.; Vendelbo, M. H.; Michalke, B.; et al. ARBM101 (Methanobactin SB2) Drains Excess Liver Copper via Biliary Excretion in Wilson's Disease Rats. Gastroenterology 2023, 165 (1), 187–200.e187.
- (31) Członkowska, A.; Litwin, T.; Dusek, P.; Ferenci, P.; Lutsenko, S.; Medici, V.; Rybakowski, J. K.; Weiss, K. H.; Schilsky, M. L. Wilson disease. *Nat. Rev. Methods Primers* **2018**, *4* (1), 21.
- (32) Tanzi, R.; Petrukhin, K.; Chernov, I.; Pellequer, J.; Wasco, W.; Ross, B.; Romano, D.; Parano, E.; Pavone, L.; Brzustowicz, L.; et al. The Wilson disease gene is a copper transporting ATPase with homology to the Menkes disease gene. *Nat. Genet.* **1993**, 5 (4), 344–350
- (33) Yu, Y.; Guerrero, C. R.; Liu, S.; Amato, N. J.; Sharma, Y.; Gupta, S.; Wang, Y. Comprehensive assessment of oxidatively induced modifications of DNA in a rat model of human Wilson's disease. *Mol. Cell. Proteomics* **2016**, *15* (3), 810–817.
- (34) Uriu-Adams, J. Y.; Keen, C. L. Copper, oxidative stress, and human health. *Mol. Aspects Med.* **2005**, 26 (4–5), 268–298.
- (35) Ogra, Y.; Chikusa, H.; Suzuki, K. T. Metabolic fate of the insoluble copper/tetrathiomolybdate complex formed in the liver of LEC rats with excess tetrathiomolybdate. *J. Inorg. Biochem.* **2000**, 78 (2), 123–128.
- (36) Zhang, L.; Lichtmannegger, J.; Summer, K. H.; Webb, S.; Pickering, I. J.; George, G. N. Tracing copper—thiomolybdate complexes in a prospective treatment for Wilson's disease. *Biochemistry* **2009**, *48* (5), 891–897.
- (37) Chen, D.-B.; Feng, L.; Lin, X.-P.; Zhang, W.; Li, F.-R.; Liang, X.-L.; Li, X.-H. Penicillamine increases free copper and enhances

- oxidative stress in the brain of toxic milk mice. PLoS One 2012, 7 (5), No. e37709.
- (38) Gitlin, J. D. Wilson disease. Gastroenterology 2003, 125 (6), 1868-1877.
- (39) Walshe, J. M. Cause of death in Wilson disease. *Mov. Disord.* **2007**, 22 (15), 2216–2220.
- (40) Weiss, K. H.; Stremmel, W. Evolving perspectives in Wilson disease: diagnosis, treatment and monitoring. *Curr. Gastroenterol. Rep.* **2012**, *14*, 1–7.
- (41) Schilsky, M. L. Liver transplantation for Wilson's disease. *Ann. N.Y. Acad. Sci.* **2014**, 1315 (1), 45–49.
- (42) Semrau, J. D.; DiSpirito, A. A.; Yoon, S. Methanotrophs and copper. FEMS Microbiol. Rev. 2010, 34 (4), 496–531.
- (43) Peng, P.; Yang, J.; DiSpirito, A. A.; Semrau, J. D. MmoD regulates soluble methane monoxygenase and methanobactin production in *Methylosinus trichosporium* OB3b. *Appl. Environ. Microbiol.* 2023, No. e01601-23, DOI: 10.1128/aem.01601-23.
- (44) Farhan Ul Haque, M.; Gu, W.; Baral, B. S.; DiSpirito, A. A.; Semrau, J. D. Carbon source regulation of gene expression in Methylosinus trichosporium OB3b. *Appl. Microbiol. Biotechnol.* **2017**, 101 (9), 3871–3879.
- (45) Smith, T. J.; Slade, S. E.; Burton, N. P.; Murrell, J. C.; Dalton, H. Improved system for protein engineering of the hydroxylase component of soluble methane monooxygenase. *Appl. Environ. Microbiol.* **2002**, *68* (11), 5265–5273.
- (46) Krentz, B. D.; Mulheron, H. J.; Semrau, J. D.; DiSpirito, A. A.; Bandow, N. L.; Haft, D. H.; Vuilleumier, S.; Murrell, J. C.; McEllistrem, M. T.; Hartsel, S. C.; Gallagher, W. H. A comparison of methanobactins from *Methylosinus trichosporium* OB3b and Methylocystis strain SB2 predicts methanobactins are synthesized from diverse peptide precursors modified to create a common core for binding and reducing copper ions. *Biochemistry* **2010**, *49* (47), 10117–10130.
- (47) Bandow, N.; Gilles, V. S.; Freesmeier, B.; Semrau, J. D.; Krentz, B.; Gallagher, W.; McEllistrem, M. T.; Hartsel, S. C.; Choi, D. W.; Hargrove, M. S.; et al. Spectral and copper binding properties of methanobactin from the facultative methanotroph *Methylocystis* strain SB2. *J. Inorg. Biochem.* **2012**, *110*, 72–82.
- (48) Dershwitz, P.; Bandow, N. L.; Yang, J.; Semrau, J. D.; McEllistrem, M. T.; Heinze, R. A.; Fonseca, M.; Ledesma, J. C.; Jennett, J. R.; DiSpirito, A. M.; et al. Oxygen generation via water splitting by a novel biogenic metal ion-binding compound. *Appl. Environ. Microbiol.* **2021**, *87* (14), e00286–00221.
- (49) Dusek, P.; Roos, P. M.; Litwin, T.; Schneider, S. A.; Flaten, T. P.; Aaseth, J. The neurotoxicity of iron, copper and manganese in Parkinson's and Wilson's diseases. *J. Trace Elem. Med. Biol.* **2015**, *31*, 193–203.
- (50) Cherny, R. A.; Atwood, C. S.; Xilinas, M. E.; Gray, D. N.; Jones, W. D.; McLean, C. A.; Barnham, K. J.; Volitakis, I.; Fraser, F. W.; Kim, Y.-S.; et al. Treatment with a copper-zinc chelator markedly and rapidly inhibits β -amyloid accumulation in Alzheimer's disease transgenic mice. *Neuron* **2001**, *30* (3), 665–676.
- (51) Bossy-Wetzel, E.; Schwarzenbacher, R.; Lipton, S. A. Molecular pathways to neurodegeneration. *Nat. Med.* **2004**, *10* (Suppl 7), S2–S9.
- (52) Scheltens, P.; De Strooper, B.; Kivipelto, M.; Holstege, H.; Chételat, G.; Teunissen, C. E.; Cummings, J.; van der Flier, W. M. Alzheimer's disease. *Lancet* **2021**, 397 (10284), 1577–1590.
- (53) Gamez, P.; Caballero, A. B. Copper in Alzheimer's disease: Implications in amyloid aggregation and neurotoxicity. *AIP Adv.* **2015**, *5* (9), No. 1, DOI: 10.1063/1.4921314.
- (54) Gaggelli, E.; Kozlowski, H.; Valensin, D.; Valensin, G. Copper homeostasis and neurodegenerative disorders (Alzheimer's, prion, and Parkinson's diseases and amyotrophic lateral sclerosis). *Chem. Rev.* **2006**, *106* (6), 1995–2044.
- (55) Brewer, G. J. Alzheimer's disease causation by copper toxicity and treatment with zinc. *Front. Aging Neurosci.* **2014**, *6*, No. 92.
- (56) Bush, A. I. Drug development based on the metals hypothesis of Alzheimer's disease. *J. Alzheimers Dis.* **2008**, *15* (2), 223–240.

- (57) Squitti, R. Copper dysfunction in Alzheimer's disease: from meta-analysis of biochemical studies to new insight into genetics. *J. Trace Elem. Med. Biol.* **2012**, *26* (2–3), 93–96.
- (58) Squitti, R.; Siotto, M.; Polimanti, R. Low-copper diet as a preventive strategy for Alzheimer's disease. *Neurobiol. Aging* **2014**, *35*, S40–S50.
- (59) Huang, X.; Atwood, C. S.; Moir, R. D.; Hartshorn, M. A.; Tanzi, R. E.; Bush, A. I. Trace metal contamination initiates the apparent auto-aggregation, amyloidosis, and oligomerization of Alzheimer's $A\beta$ peptides. *JBIC*, *J. Biol. Inorg. Chem.* **2004**, *9*, 954–960.
- (60) Miller, L. M.; Wang, Q.; Telivala, T. P.; Smith, R. J.; Lanzirotti, A.; Miklossy, J. Synchrotron-based infrared and X-ray imaging shows focalized accumulation of Cu and Zn co-localized with β -amyloid deposits in Alzheimer's disease. *J. Struct. Biol.* **2006**, *155* (1), 30–37.
- (61) Whittenbury, R.; Phillips, K.; Wilkinson, J. Enrichment, isolation and some properties of methane-utilizing bacteria. *Microbiology* **1970**, *61* (2), 205–218.
- (62) LaFleur, T. L.; Hossain, A.; Salis, H. M. Automated model-predictive design of synthetic promoters to control transcriptional profiles in bacteria. *Nat. Commun.* **2022**, *13* (1), No. 5159.
- (63) Reis, A. C.; Salis, H. M. An automated model test system for systematic development and improvement of gene expression models. *ACS Synth. Biol.* **2020**, *9* (11), 3145–3156.
- (64) Welander, P. V.; Summons, R. E. Discovery, taxonomic distribution, and phenotypic characterization of a gene required for 3-methylhopanoid production. *Proc. Natl. Acad. Sci. U.S.A.* **2012**, *109* (32), 12905–12910.
- (65) Schäfer, A.; Tauch, A.; Jäger, W.; Kalinowski, J.; Thierbach, G.; Pühler, A. Small mobilizable multi-purpose cloning vectors derived from the *Escherichia coli* plasmids pK18 and pK19: selection of defined deletions in the chromosome of *Corynebacterium glutamicum*. *Gene* **1994**, 145 (1), 69–73.
- (66) Simon, R. High frequency mobilization of gram-negative bacterial replicons by the in vitro constructed Tn 5-Mob transposon. *Mol. Gen. Genet.* **1984**, *196* (3), 413–420.
- (67) Martin, H.; Murrell, J. Methane monooxygenase mutants of *Methylosinus trichosporium* constructed by marker-exchange mutagenesis. *FEMS Microbiol. Lett.* **1995**, *127* (3), 243–248.
- (68) Peng, P.; Zheng, Y.; Koehorst, J. J.; Schaap, P. J.; Stams, A. J.; Smidt, H.; Atashgahi, S. Concurrent haloalkanoate degradation and chlorate reduction by *Pseudomonas chloritidismutans* AW-1^T. *Appl. Environ. Microbiol.* **2017**, 83 (12), e00325–00317.